What Controls Activity Trends of Electrocatalytic Hydrogen Evolution Reaction?—Activation Energy *Versus* Frequency Factor

Aleksandar R. Zeradjanin,* Praveen Narangoda, Justus Masa, and Robert Schlögl

ACCESS | Metrics & More | Article Recommendations | SI Supporting Information

ABSTRACT: Renewable energy storage *via* water electrolysis strongly depends on the design of electrified electrode−electrolyte interfaces at which electricity is converted into chemical energy. At the core of the hydrogen evolution reaction (HER) and the oxygen evolution reaction conversion efficiency are interfacial processes with complex dynamic mechanisms, whose further acceleration is practically impossible without a thorough fundamental understanding of electrocatalysis. Here, we communicate new experimental insights into HER, which will potentially further deepen our general understanding of electrocatalysis. Of special note is the very surprising observation that the most active metals (*i.e.*, noble metals) for HER, which exhibit the lowest overpotentials at a defined current density, exhibit the highest activation energies in comparison to the other metals from the d-block. This suggests a major, if not dominant, impact of the frequency factor on activity trends and the need for deeper reconsideration of the origins of electrocatalytic activity.
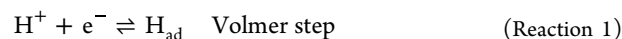
KEYWORDS: electrocatalysis, water splitting, hydrogen evolution, activation energy, pre-exponential factor
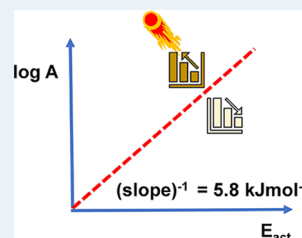
1. INTRODUCTION

One of the most appealing strategies for enhancing global utilization of clean and sustainable energy is to store renewable electricity in chemical bonds.[1] At the frontiers of scientific and technical development toward realizing this goal are challenges related to water electrolysis, in which two electrified electrode−electrolyte interfaces are functionalized to split water into molecular hydrogen at the cathode and molecular oxygen at the anode.[2,3] During the last decade, the number of published papers related to water electrolysis is difficult to count, of which a significant portion is dedicated to the comparatively more complex oxygen evolution reaction (OER).[4] Being significantly more sluggish and more corrosive in comparison to the hydrogen evolution reaction (HER), the OER is perceived as a key challenge in the implementation of efficient water electrolyzers.[5] Without undermining the tremendous scientific efforts and progress made in the quest for new OER catalyst materials, an often overlooked problem is that despite the HER being comparatively better understood than the OER, many dynamic aspects of the HER mechanism remain unknown, including the exact, probably multifunctional, role of water molecules.[6,7] The unusual complexity of the HER indicates that the current fundamental understanding of electrocatalysis is insufficient to explain reaction mechanisms and inspire rational catalyst design.[8] Ordinarily, the conventional theory of electrocatalysis is based on the paradigm of the Sabatier principle, an intuitive notion that considers optimal (not too strong, not too weak) binding of intermediates as a prerequisite for a high reaction rate.[9,10] Key emphasis is on the thermodynamics of adsorption,[11] even in the case of complex multielectron reactions,[12] independently from that are the pathways homolytic

or heterolytic[13,14] and independent from that is it multielectron reaction proceeding on metal surfaces or metals with incorporated ligands (*e.g.*, MN4) and so forth.[15] Applied to the HER, it means that the intermediate (Had) formed in the first elementary step (Volmer step) should have moderate adsorption strength.[16,17] If Had is bonded too strongly, then H2 molecule formation through the recombination processes (Reaction 2a and Reaction 2b) will be sluggish; conversely, if Had is bonded too weakly, the proton will desorb from the catalyst surface before the product is generated.
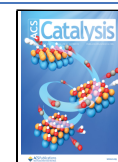
$$H^+ + e^- \rightleftharpoons H_{ad} \quad \text{Volmer step} \tag{Reaction 1}$$

$$H_{ad} + H^+ + e^- \rightleftharpoons H_2 \quad \text{Heyrovsky step} \tag{Reaction}$$

$$2H_{ad} \rightleftharpoons H_2 \quad \text{Tafel step} \tag{Reaction}$$

In more quantitative terms, the exchange current (j_0—reaction rate at equilibrium potential) is essentially determined by the adsorption energy of the intermediate formation, as illustrated with eq 1[18]

$$j_0 = nFc^p(H^+)(1-\theta)^q k_{et} \, \exp\left(\frac{-\beta F E_{rev}}{RT}\right) \exp\left(\frac{-\gamma \Delta G_{ad}}{RT}\right) \tag{1}$$
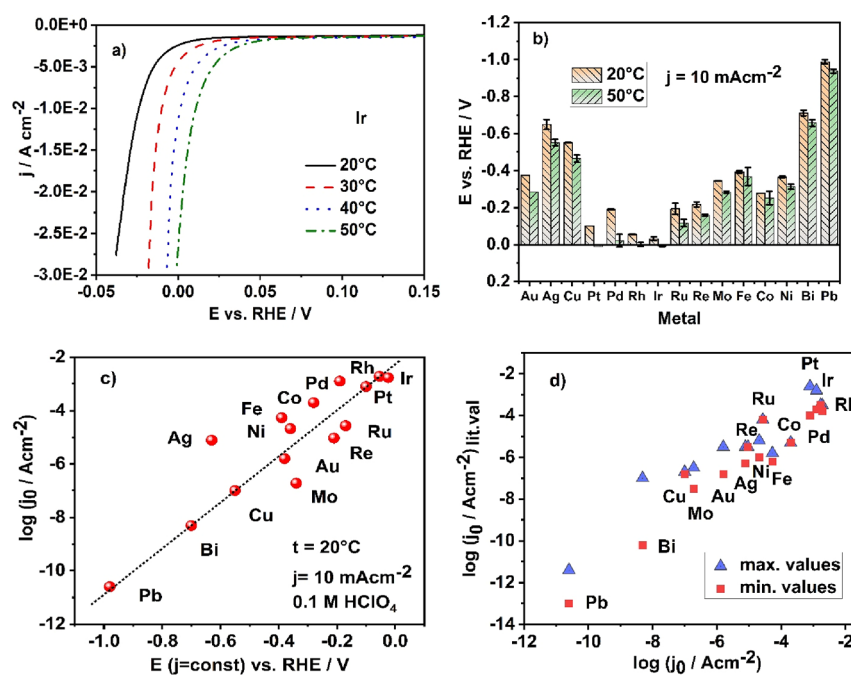
Figure 1. (a) Example of Ohmic drop-corrected HER polarization curves for Ir in 0.1 M HClO$_4$ at four different temperatures, recorded using hydrodynamic LSV using a scan rate of 5 mV s^{-1} with 1600 rpm. The polarization curves for the other metals were recorded under identical conditions from which the potential at a current density of 10 mA cm^{-2} was extracted, as shown in the Supporting Information; (b) activity trends at temperatures of 20 and 50 °C for 15 metals. (c) Potentials at constant HER current density (b) of 10 mA cm^{-2} in relation to HER exchange current densities and (d) HER exchange current densities from our lab in relation to HER exchange current densities from well-established literature sources (from ref 16). The red rectangles indicate minimum literature values of HER exchange currents, while the blue triangles indicate maximal values of exchange currents.

where n is the number of exchanged electrons, F is Faraday's constant, $c(H^+)$ is the concentration of protons, p is the partial order with respect to proton concentration, θ is total coverage, q is the partial order with respect to the number of available active sites, k_{et} is the electron transfer rate constant, β is the symmetry factor, E_{rev} is reversible potential, R is the universal gas constant, T is temperature, ΔG_{ad} is adsorption energy of intermediate formation, and γ is the Brönsted–Evans–Polanyi (BEP) coefficient. The resulting log j_0 versus ΔG_{ad} dependence for the HER on various metals yields a volcano-type plot, where the activation and pre-exponential (frequency) terms in eq 1 are balancing each other. Balance is established by the competition of ΔG_{ad} versus $(1 - \theta)$, where for very exergonic adsorption, the resulting activation energy should be very low while the coverage should be very high. Conversely, for very endergonic adsorption, the resulting activation energy should be high while coverage should be low. The HER exchange current has its highest value when H$_{ad}$ formation is thermoneutral and entropy-driven (ΔG_{ad} = 0), which corresponds to the "volcano" apex.[7,8,11,13] Activity trends based on this assumption are nowadays widely accepted, but were in the past critically discussed by experimentalists and theoreticians.[8,19] There were indications that the top of the "volcano" can be shifted toward weaker hydrogen binding with respect to thermoneutral conditions,[8] which has gained increasing acceptance in recent years.[20–22] Besides the "volcano" plot, the free energy relation for HER (log j_0 vs ΔG_{ad}) could also be linear.[8,19,23] Finally, independently from what is more correct ("volcano" or "linear plot"), the key important observation is that intermediate adsorption free energy as one single parameter is definitely insufficient to explain activity,[6,24,25] which should be straightforward from the rate law (eq 1). Based on this observation and on the existence of a direct link between the adsorption energy of intermediates (eq 1) and

activation energy for HER, we come to the critical question: is activation energy really the determinant factor controlling HER activity trends, as widely believed for decades?

2. RESULTS AND DISCUSSION

2.1. Why Reconsider Origins of Electrocatalytic Activity? If one analyzes eq 1, it becomes evident that the reaction rate depends on several complex kinetic parameters. Inherent experimental difficulties during the estimation of kinetic parameters[26] as well as variations in the values of the kinetic parameters determined on different experimental setups, bring into question any kinetic analysis of HER. Even seminal contributions like the works of Trasatti contain data collected under nonidentical conditions.[16] This is even more relevant in the case of high-temperature HER experiments necessary for the estimation of activation energy. What is encouraging is the experimental fact that HER activity trends based on a comparison of exchange currents obtained by different authors and on different experimental setups generally agree with each other.[27] Nevertheless, kinetic data on HER for a significant number of metallic catalysts obtained under identical conditions is difficult to find in the literature, especially if we analyze kinetic parameters other than exchange current. Therefore, despite the fact that the HER has been investigated for decades, it was important to conduct experiments with a significant number of samples under identical conditions and compare the results on exchange currents with literature data to make the analysis of the activity trends truly relevant. We conducted an investigation of the HER on 14 d-metals and two sp-metals at various temperatures by conducting pseudo-stationary linear sweep voltammetry (LSV) with a sweep rate of 5 mV s^{-1} up to a potential where a current density of 25 mA cm^{-2} is reached. The utilized sweep rate was appropriate because there was no

expectation for the diffusion of reactants/products (*e.g.,* protons) into the "inner" regions of the electrode surface, as could be the case for thick porous electrode materials like oxides,[28] mixed oxides,[29] and/or metal nanoparticles decorated polymers.[30] The utilized catalysts were polycrystalline metallic discs with a thickness of 3 mm and a diameter of 5 mm. The purity of the metals was from 99.9% (*e.g.,* Ru) up to 99.999% (*e.g.,* Bi), which were pretreated using the same procedure (given in the Experimental Section), so differences in roughness are expected to be minor. An example of LSVs on Ir at four different temperatures is given in Figure 1a.

In contrast to our initial experiments that were done in alkaline electrolyte,[31] experiments shown in this work were conducted in the acidic electrolyte (*i.e.,* 0.1 M HClO$_4$). The reason for this is that impurities in the form of various anions (*e.g.,* chlorides) desorb to a great extent as we approach from open circuit potential (OCP) toward the reversible potential for HER.[32] The situation is opposite in alkaline media, where impurities in the form of cations (*e.g.,* Fe in KOH-based electrolytes) could be deposited at potentials where HER proceeds, altering the kinetics of water activation and hydrogen adsorption,[33] and consequently the electrocatalytic activity.[34]

Activity trends in this work were obtained by comparison of the potentials at a current density of 10 mA cm^{-2} (Figure 1b), and relating this to the exchange currents (Figure 1c), which are finally correlated with well-established literature values for exchange currents (Figure 1d). In this way, we corroborate the credibility of our experimental results. The extent of the overlap between the literature values and our values is excellent. Evidently, the noble metals were the most active as reported in numerous works.[16,17] It should not be surprising that HER potential is more positive than 0 V *versus* RHE for some noble metals. An example of this phenomenon was shown previously by Jerkiewicz, in a case of Pt at which HER in argon saturated electrolytes was observed to commence at potentials at least 50 mV more positive than 0 V *versus* RHE.[35] In our case, Pt was the third most active metal after Ir and Rh (Figure 1b). Ir was previously reported to be the most active metal for HER in alkaline media,[36] but if one carefully analyzes literature data sets on exchange current for HER in acidic media, it is well-known that noble metals exhibit minor differences in exchange current, and that Pt does not have to be the most active, as generally perceived. By comparing the logarithm of exchange current for HER in acidic media on noble metals from well-established literature sources[16] [Ir (−3.5), Rh (from −3.5 to −3.8), Pt (from −2.6 to −4.0), Pd (from −2.8 to −3.7), Re (from −3.0 to −5.5), and Ru (−4.2)], it becomes apparent, with the exception of Ru, that any of the discussed noble metals (Ir, Rh, Pd, and Re) could exhibit higher activity in comparison to Pt, which depends on the nature of counter anions in acidic media, purity of the electrode, and purity of the electrolyte, among others. At 20 °C, the activity difference between Ir, Rh, and Pt, although modest, is evident while at 50 °C, the activity difference between the three metals almost completely vanished. The activity of the metals at 20 °C was in the order: Ir > Rh > Pt > Ru > Pd > Re > Co > Mo > Ni > Au > Fe > Cu > Ag > (Bi) > (Pb) > Mn; at 50 °C, the activity trend was: Ir > Pt > Rh > Pd > Ru > Re > Co > Mo > Ni > Au > Fe > Cu > Ag > (Bi) > (Pb) > Mn. If the activity trends at the two temperatures are compared, the exact order of the five most active metals slightly changed (Pt and Rh exchanged positions and Pd and Ru exchanged positions), while it was literally identical for the other metals. It is important to stress that the polarization curves of Mn were completely linear,

indicating the formation of very insulating oxide layers in contact with the electrolyte. The OCP after immersion of Mn in the electrolyte was −1.3 V *versus* RHE, suggesting that Mn was the least active of the tested metals, even less active than the sp-metals (Bi, Pb), which very weakly adsorb protons. It is reasonable for one to ask whether oxides are formed on the surface of the 3d metals (*i.e.,* Fe, Co, Ni). To be absolutely sure on this issue, we would need to apply *in situ* or in-operando spectroscopies. However, spectroscopy probes only a small fraction of the electrocatalyst surface and practically gives information which cannot exclude the local existence of oxide on some other parts of the surface. Our approach, if we take the example of Fe as the most nonnoble 3d metal used, assumes that at potentials of 0 V and at pH = 1 (from Pourbaix diagrams), involves only active dissolution of Fe, including dissolution of eventually formed oxide. Therefore, HER will not be significantly influenced by previously formed oxide in the used potential range. The electrodes were kept at OCP for 15 min before applying LSVs from 0.1 V *versus* RHE toward a potential where 25 mA cm^{-2} was reached. The initial point of the LSV, with a potential of 0.1 V, was more positive than the OCP only in the cases of Fe, Co, and Pb. Fe had the most negative OCP, at around −0.2 V *versus* RHE. So at 0.1 V *versus* RHE, where Fe is thermodynamically unstable, we will just accelerate Fe dissolution in comparison to OCP, but then soon after sweeping the potential from 0.1 V toward −0.2 V *versus* RHE and further, HER will dominate as the main reaction with only a minor contribution, if any, of Fe redeposition. Also linked to this, directly or indirectly, is the question of the active surface area. For decades, numerous methods were developed to count active sites or electrochemically active surface areas on different classes of materials (*i.e.,* metals, alloys, oxides, *etc.*). However, none of them is universal. Especially, there is a tendency to utilize the capacitance of the double layer obtained by impedance spectroscopy (or cyclic voltammetry) as a universal method to estimate electrochemically active surface area. The challenge with this approach is that the specific capacitance of various metal/electrolyte interfaces (usually estimated for low index single crystal metal surfaces) will be significantly different for different metals. The situation becomes even more complicated when we have polycrystalline metals with a nonquantifiable number of defects. For the sake of simplicity, flat polycrystalline electrodes were used, which were pretreated using the same procedure described in the Experimental Section, so differences in surface roughness between different metals are expected to be minor. However, even if we could accurately determine the number of active sites for gas evolving electrodes, that would still not be sufficient. What is most relevant is the effective surface area, that is somewhere between the real area (defined by the total number of active sites) and the geometric area. Effective surface area is the average fraction of the real surface area that is not covered by gas bubbles at a defined overpotential. We proposed in the past a methodology to estimate that quantity; however, the methodology conceals some weak points.[26,37,38] To our knowledge, a reliable methodology for determining effective surface area is yet to be developed; until then, every comparison or kinetic analysis of gas evolving electrodes done in the last 100 years is questionable. This is also valid for flat electrodes (not only for porous electrodes) because gas evolution depends on the hydrophilicity/hydrophobicity of a surface that can significantly vary on different metals, oxides, and so forth of flat surfaces. Considering gas evolving electrodes like electrocatalytic electrodes for HER, and the phenomenon of gas
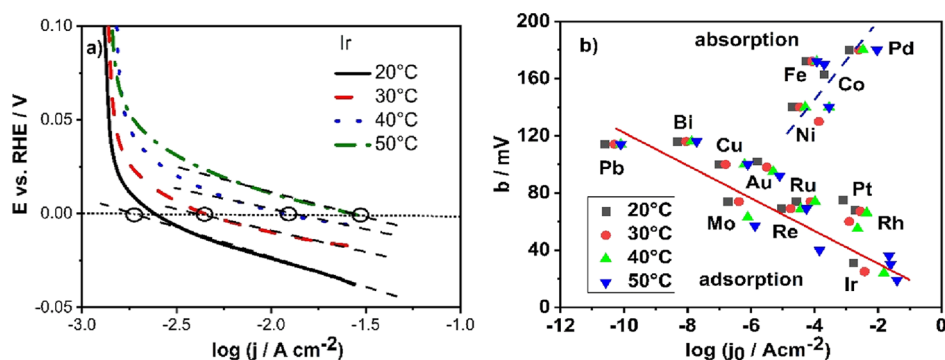
Figure 2. (a) Example of the Tafel plot for HER on Ir in 0.1 M HClO$_4$, from which exchange currents and Tafel slopes were extracted at four different temperatures. The current range was approximately 1 order of magnitude (between −1.5 and −2.5), dotted line indicated reversible potential, and four black circles were used to mark the point of the extrapolated linear part of the polarization curve on reversible potential. (b) Relation between Tafel slope and exchange current for metals exhibiting adsorption (full red line) and for metals exhibiting absorption (blue-dashed line). The plot was compiled for four temperatures: 20 °C (black cubes), 30 °C (red circles), 40 °C (green triangles), and 50 °C (blue inversed triangles). The Tafel slope for hydrogen adsorbing metals strongly negatively correlate with exchange current, with a correlation coefficient of $r = -0.85$. For hydrogen absorbing metals, the correlation is moderately strongly positive with a correlation coefficient of $r = 0.64$.

blockage of active sites, it is important to be aware of the following facts: increase of overpotential increases the interfacial concentration of hydrogen, which accelerates gas-bubble nucleation, coalescence, and growth as well as detachment. This defines the effective surface area as a dynamic property that fluctuates but with a certain average value at a defined overpotential. Despite of the applied rotation by rotating disc electrode (RDE), some nanobubbles periodically block active sites, which will introduce uncertainty into $(1 - \theta)$ term if we consider eq 1. In other words, $(1 - \theta)$ that indicates the number of available active sites should be $(1 - \theta) = (1 - \theta_H - \theta_{bubbles})$, evidently lower than that in the absence of gas evolution. The impact is that the estimated/measured current density during potentiostatic polarization, including the pre-exponential factor, is actually lower, because the actual number of available active sites is lower than $(1 - \theta_H)$ suggests. Accurately determining the effective surface is a major methodological challenge for electrocatalysis, as shown in our previous work, where we proposed the combination of CV, amperometry, and local electrochemical noise measured by SECM. Admittedly, the challenge of reliably determining effective surface area at gas evolving electrodes introduces uncertainty of an unknown magnitude into all electrochemical measurements on gas evolving electrodes during the last 100 years. In the current work, we attempted to estimate the change in the double layer capacitance at 100 kHz, using the Mott−Schottky module of electrochemical impedance spectroscopy (EIS) by comparing the potential region where no gas bubbles were generated with the potential region(s) where bubbles were generated. However, the experiments were coupled with substantial noise. An illustrative example of this with additional discussion is given in the Supporting Information. Everything shown here demonstrates that our data on exchange currents were collected in a reasonable manner, consistent with relevant literature sources, suggesting that data obtained at elevated temperatures should be reliable.

2.2. Close to Equilibrium *Versus* Far from Equilibrium Activity Trends. As we move from the equilibrium potential, besides exchange current, the Tafel slope (b) becomes increasingly relevant for overall activity. The Tafel slope depicts how flexibly one can alter the activation barrier with electrode potential, and it is primarily a function of the symmetry factor (eq 1) that gives certain insight into the shape of the activation

barrier. Computational chemists usually focus only on exchange current and ignore the Tafel slope, because the symmetry factor and Tafel slope cannot be easily computed.[17] The reason for this is that, up to date, it is not straightforward what electrocatalyst or electrode/electrolyte interface properties determine the value of the symmetry factor.[39] The dependence of overpotential, as the most complex kinetic parameter, on exchange current and Tafel slope is given by eq 2.

$$\eta = b \, \log \frac{j}{j_o} \tag{2}$$

where η is overpotential at a defined current density and j is current density. In general terms, for one electrocatalytic electrode (*i.e.*, metal), the overpotential is directly proportional to the Tafel slope and inversely proportional to exchange current. In other words, at a defined overpotential, the obtained reaction rate (measured current density) will depend on the intrinsic relation between exchange current and Tafel slope. For single metals, it is straightforward to understand how exchange current and Tafel slope influence overpotential; a more general phenomenological quantitative relation between exchange currents and Tafel slopes for HER on various metals (*e.g.*, d-metals) has never been analyzed to date. Figure 2 shows a relationship between exchange current and Tafel slope, two fundamental kinetic parameters that are controlling the reaction rate close to equilibrium and far from equilibrium, respectively. Exchange current and Tafel slope were obtained from the Tafel plots (plots *E vs* log j) with the example of Ir shown in Figure 2a. Knowing that Tafel plots for one electrode reaction on different electrocatalysts could intersect,[40] it is surprising that for the set of the analyzed metals, exchange current densities and Tafel slopes are almost exclusively inversely proportional. In other words, close-to-equilibrium and far-from-equilibrium, HER activity trends in acidic media are practically identical. This is valid for all metals exhibiting surface adsorption, for which the maximum Tafel slope was around 120 mV/dec. However, four metals, Pd and the iron triad (Fe, Co, and Ni) exhibited opposite behavior.[41] These metals, known by their ability to absorb hydrogen into the metal bulk and form hydrides,[42] showed a tendency where the Tafel slope increases with an increase of exchange current. In this case, the Tafel slope is above 120 mV/dec, indicating involvement of bulk reactions. For this study,
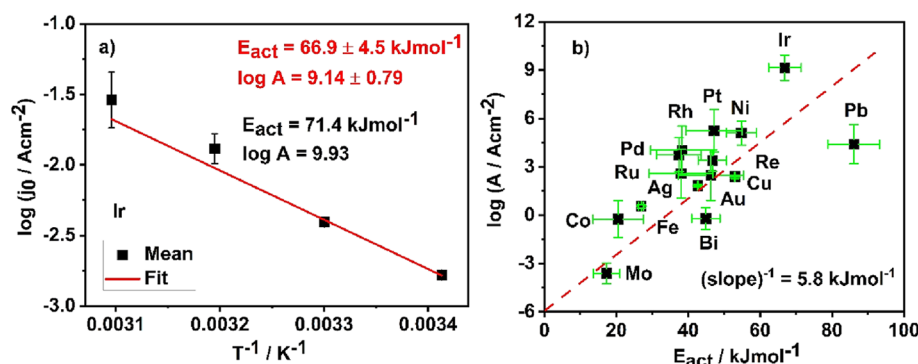
Figure 3. (a) Example of the Arrhenius plot for HER on Ir in 0.1 M HClO$_4$. Arrhenius plots of the other 14 metals are given in the Supporting Information. Values of the fit area are marked with red, while preferential values of parameters are marked with black. (b) Relation between activation energy (E_{act}) and the logarithm of pre-exponential factor (log A) as an illustration of the compensation effect for HER in acidic media. Error bars originate from exchange currents estimated at the beginning of experimental protocol and the exchange currents were estimated at the end of the experimental protocol (approximately after 1 h). Linear fit was based on experimental points collected at all four temperatures. A similar dependence was obtained if three data points were utilized for the fit, excluding the data point at 50 °C as well as in the case of extrapolation of the linear dependence based on four data points plotted manually without fitting.

current densities of tens of mA cm^{-2} determined using RDE were used. Future studies should use membrane electrode assemblies, enabling hundreds of mA cm^{-2} to be investigated.

For both groups of metals, (*i.e.*, adsorbing and absorbing metals), the intrinsic reasons for the direct link between Tafel slope and exchange current are not clear, although a phenomenological link evidently exists. The increase of exchange current by an order of magnitude, in the case of metals that adsorb protons, is coupled with a reduction of Tafel slope by approximately 10 mV, while there was a coupled increase of the Tafel slope by approximately 30 mV in the case of metals that absorb protons. Importantly, if exchange currents and Tafel slopes follow the dependence shown in Figure 2b, then in the first approximation, it is sufficient to focus on electrocatalytic activity trends close-to-equilibrium by resolving intrinsic limitations of exchange current, which is quite the opposite to alkaline media, where it is necessarily to consider the behavior of HER also far-from-equilibrium.[31]

2.3. Activation Energy *Versus* Frequency Factor. To analyze the key determinants of exchange current, it was necessary to utilize the Arrhenius equation, or in other words, to investigate the temperature dependence of exchange current to obtain the activation energy (E_{act}) and pre-exponential (frequency) factor (A) as well as their mutual relation. The most general equation for reaction rate in electrochemistry suggests a direct relation between current density and (over)potential dependent rate constant (k) and concentration of all reactants ($\prod_i c_i^R$). The equation is relevant for the rate-determining step (eq 3)

$$j = nF \prod_i c_i^R k \tag{3}$$

Arrhenius equation (eq 4) gives the temperature dependence of the rate constant of any chemical reaction

$$k = A_{freq} \exp\left(\frac{-E_{act}}{RT}\right) \tag{4}$$

where A_{freq} is collision frequency. Activation energy is actually enthalpy that comprises free energy of activation (ΔG_{act}) and activation entropy (ΔS_{act}). For electrocatalytic reactions like HER, the free energy of activation depends on the standard free energy of activation (ΔG^*), the electrode potential, and the

adsorption energy of intermediate formation (ΔG_{ad}). Then the rate constant becomes

$$k = A_{freq} \exp\left(\frac{-\Delta S_{act}}{R}\right) \exp\left(\frac{-\Delta G^*}{RT}\right) \exp\left(\frac{-\beta FE}{RT}\right) \\ \exp\left(\frac{-\gamma \Delta G_{ad}}{RT}\right) \tag{5}$$

By plugging the rate constant (eq 5) into the equation for current density (eq 3), where reactants are protons capable of adsorbing on available active sites at metal surfaces (sites not already occupied by intermediates) accessible for adsorption, we obtain eq 6

$$j = nFc^p(H^+)(1 - \theta)^q A_{freq} \exp\left(\frac{-\Delta S_{act}}{R}\right) \exp\left(\frac{-\Delta G^*}{RT}\right) \\ \exp\left(\frac{-\beta FE}{RT}\right) \exp\left(\frac{-\gamma \Delta G_{ad}}{RT}\right) \tag{6}$$

All the quantities are as previously defined in the text. If we are at reversible potential and we transform the reaction rate (eq 6) into a semilogarithmic relation, we get

$$\log j_0 = \log\left(nFc^p(H^+)(1 - \theta)^q A_{freq}\right) \\ + \frac{1}{2.303}\left(\frac{-\Delta S_{act}}{R} + \frac{-\Delta G^*}{RT} + \frac{-\beta FE_{rev}}{RT} \right. \\ \left. + \frac{-\gamma \Delta G_{ad}}{RT}\right) \tag{7}$$

Finally, we obtain a form of the equation that is relevant for the experimental work (eq 8)

$$\log j_0 = \log A - \frac{E_{act}}{2.303RT} \tag{8}$$

While activation energy is independent of the number of active sites, from eq 7, one can notice how gas-bubble blockage influences the pre-exponential frequency factor through the $(1 - \theta)$ term, causing inaccuracy in determining accurate values of rate constants. In other words, to determine the value of the rate

constant, it is necessary to know partial orders of reactant with respect to protons (p), total coverage (θ), including coverage with intermediate (θ_H), and coverage with gas bubbles ($\theta_{bubbles}$), as well as partial order of the reaction with respect to the number of available active sites (q), which is very complex. Therefore, we focused on the analysis of the total pre-exponential frequency factor that includes all these parameters and analysis of the total activation energy for different metals. Importantly, from eq 7, the link between activation energy and adsorption energy is straightforward; however, it also indicates that direct linear relations between adsorption energy and activation energy, known in heterogenous thermal catalysis as BEP relations, are possibly oversimplifications in the case of electrocatalytic reactions. The paradigm followed for 70 years (from the works of Parsons[9] and Gerischer[43] in 1950s) in electrocatalysis of HER, that reducing activation energy by tuning of intermediate adsorption will enhance HER activity, seems reasonable; however, it lacks solid grounding in consistent experimental data. The first underlying question is: does activation energy control HER activity trends and how realistic is the perspective to further accelerate the HER by reducing the activation energy? An example of activation energy and pre-exponential factor determination on Ir is illustrated in Figure 3a ($\log j_0$ vs $1/T$), having in mind eqs Reaction 1−5. Practically, the slope of the inverse temperature dependence of exchange current comprises activation energy, while the intercept (i.e., extrapolation of exchange current to infinite temperature) is equal to logarithm of the pre-exponential factor. For the example of Ir, the correlation is strongly negative with a correlation coefficient of −0.997. For 13 metals, the linear fit was with a correlation coefficient above −0.9, indicating a strongly negative correlation. The only two metals where the linear fit was not possible were Ag and Cu. In the case of Cu, mean values of the data points for exchange currents were distributed in a way that a linear dependence was possible to draw intuitively; still linear fitting with sufficiently strong correlation coefficient (desirably above 0.75, or minimum 0.5) was not possible due to values of standard deviations of exchange currents data points. In the case of Ag, the linear fit yielded a relationship that suggests the so-called negative activation energy. So, the data points for these two metals were taken as not being particularly reliable. Arrhenius plots for all the 15 metals are given in the Supporting Information. The pre-exponential frequency factor was analyzed only by Schmickler et al.[44] where they examined (1) the general importance of the pre-exponential factor in electrochemistry including HER as an example of electrocatalytic reaction; (2) some possible explanations about factors that influence the pre-exponential factor based on only a few metals measured in different laboratories; and (3) the discrepancy in results of high-temperature electrochemistry on Pt between different research groups and the suggestion that experimentalists should make a substantial effort in obtaining more relevant results and that the pre-exponential factor should be investigated more thoroughly in electrocatalysis. Therefore, a significant step forward would be to (1) examine phenomenologically the relation between activation energy and pre-exponential factor on a significant number of HER electrocatalysts under identical experimental conditions; (2) accurately determine where the most active metals (noble metals) are positioned and (3) which metals have the lowest activation energies and which ones have the highest pre-exponential factor, and if possible, (4) establish whether HER electrocatalytic activity is controlled predominantly by activation energy or by pre-exponential factor.

In Figure 3b, to our knowledge, an illustration of the correlation between activation energy and pre-exponential factor for HER in acidic media is given for the first time. The two quantities are strongly corelated with a correlation factor of above 0.83. The interrelation between the exponential factor (activation energy) in the rate law and the pre-exponential (frequency) factor in thermal catalysis is known as a compensation effect and formally correlates activation enthalpy and activation entropy.[45] Therefore, the relation shown in Figure 3b can be understood also as an example of the compensation effect in HER electrocatalysis. From the inverse value of the slope in Figure 3b, it seems that the reduction of activation energy by approximately 5.8 kJ mol^{-1} is coupled with a drop in the frequency factor by an order of magnitude. The slope of E_a versus $\log A$ dependence is almost identical to the value we obtained in alkaline media,[31] indicating some universal limitation to HER kinetics that was not revealed until now. Drawing from thermal catalysis, the compensation effect in electrocatalytic HER could be understood as an interplay between the adsorption energy (ΔG_{ad}), which is related linearly with activation energy via the BEP relation and the number of available active sites at an electrocatalyst surface ($1 - \theta$).[45] The stronger the adsorption is, the larger will be the exponential factor, while the number of available active sites will be low, thus reducing the pre-exponential factor. The converse arises if the adsorption becomes weaker. From that point of view, it seems that the compensation effect is at the very root of the Sabatier principle. However, careful inspection revealed that Figure 3b is questioning the classic explanation as well as the essence of the conventional view on electrocatalysis. Notably, according to the results in Figure 3b, the most active metals for HER electrocatalysis have the highest activation energies. There is no literature source, to the best of our knowledge, that considers this reality. Despite the very low activation energy on Pt reported by Marković et al.,[46] our results are similar to the result recently reported by Schmickler et al.[47] Importantly, our results suggest that the high HER activity of noble metals in acidic electrolytes strongly depends on the pre-exponential frequency factor. If one observes that the pre-exponential factor for the different metals is spread over 12 orders of magnitude, it is clear that the explanation for that cannot be ascribed to the ($1 - \theta$) term (see eq 1). Evidently, some other phenomena that manifest themselves through the pre-exponential frequency factor other than adsorption energy have to be responsible for the electrocatalytic activity by considerably increasing the effective collisions between the reactants and the electrocatalyst surface. It therefore seems that the usual approach aiming to reduce activation energy by tuning the adsorption energies of key intermediates as a way to enhance electrocatalytic activity can be challenged. To our knowledge, no one showed this in the literature before. These are very important results and conclusions pointing out, after more than 70 years of conceptual research on HER, that electrocatalysts for HER should be designed by including a different kind of paradigm.

2.4. Need for New Type of Structure−Activity Relations. Taking into consideration that the scope of electrocatalysis is to establish a correlation(s) between properties of electrocatalytic materials and reaction rate, the conventional view that correlates the relative position of the metal d-band center (with respect to the Fermi level) with the exchange current density seems reasonable.[17] However, exchange current is a very complex quantity dependent on the activation factor and frequency factor, each influenced by several parameters.[31]

So instead of linking one electrocatalytic property of a material with reaction rate (or exchange current), it would be necessary to make dissection of activation energy and especially important to make dissection of the pre-exponential frequency factor to obtain a more vivid picture of the structure and dynamics of the electrified interface (*i.e.,* interaction of electrode with electrolyte with/without applied overpotential) and to correlate single properties of electrocatalytic materials or interfaces to single parameters in the rate law as shown in (eq 1 and/or eq 8).[48]

3. CONCLUSIONS

In summary, we showed that close-to-equilibrium and far-from-equilibrium, activity trends for HER follow the same pattern for most metals except for those with a tendency to absorb hydrogen in the bulk. In other words, we showed that despite Tafel slope as a kinetic parameter that could lead to distorted activity trends far from equilibrium, this does not happen with metals that adsorb hydrogen and exhibit negligible or no bulk absorption. However, it is shown from high-temperature electrochemistry that the most active metals (*i.e.,* noble metals) have the highest activation energies among the tested d-metals. Notably, the assumption postulated by theoreticians that noble metals adsorb intermediates with optimal bond strengths and activation energy minima is not the pattern that manifests universally in the experiment. In fact, the high activity of noble metals strongly depends on the pre-exponential frequency factor, which spans 12 orders of magnitude for different metals. Thus, the significant differences in the frequency factor for the different metals cannot be explained by the $(1 - \theta)$ term but has to be attributed to some inherent material or interfacial property that until now has not been explicitly considered of much relevance for electrocatalytic reactions, although it has a major impact on the reaction rate.

4. EXPERIMENTAL SECTION

4.1. Electrochemical Cell, Electrodes, and Electrolyte. Electrochemical measurements were conducted in a home-made temperature-controlled electrochemical cell constructed out of polyether ether ketone. Working electrodes were 16 polycrystalline metals (MaTeck, Juelich, Germany) with a thickness of 3 mm and a diameter of 5 mm, polished using SiC papers (400, 800, 1200, and 4000 grit) and alumina paste (1.0−0.05 μm), washed with 1 M KOH, followed by de-ionized water and immediately dried under a stream of argon and finally inserted into a Teflon holder as an RDE tip controlled by a rotator (Autolab, Metrohm, Switzerland) at 1600 rotations per min. The purity of the metals was from 99.9% (*e.g.,* Ru) up to 99.999% (*e.g.,* Bi). The potential of the working electrode was controlled using a potentiostat/galvanostat (BioLogic, VSP with EIS, France). The counter electrode was a graphite rod, and the reference electrode was commercial Ag/AgCl with saturated KCl (Metrohm AG, Herisau, Switzerland). Temperature was controlled with a thermostat (Huber CC-K6, Germany) in the 293−323 K range. The temperature drift of the reference electrode *versus* RHE was 0.125 mV/°C. The electrolyte was 0.1 M $HClO_4$ made by dilution out of suprapure 70% $HClO_4$ (Merck, Darmstadt, Germany) and ultrapure deionized water (ELGA, PURELAB flex system with a resistivity of 18.2 MΩ cm, Celle, Germany). The electrolyte was pretreated by electrolysis over a duration of 30 min at 10 mA cm^{-2} to minimize the impact of impurities (especially chlorides, but also incidental organic impurities, *etc.*).

4.2. LSV, Tafel Analysis, and Arrhenius Plots. After an initial 15 min of OCP, polarization curves were recorded in the potential range from 0.1 V *versus* RHE up to a potential where a current density of 25 mA cm^{-2} was reached with a scan rate of 5 mV s^{-1}. From the Ohmic drop-corrected polarization curves, Tafel analysis was conducted by linear regression of Tafel plots to the reversible potential of HER. The applied current range was from −2.5 mA cm^{-2} up to −25 mA cm^{-2}. It is an order of magnitude change in the current range, practically the minimum that is required to apply Tafel's analysis. If we take the example of Pt, there are two linear regions. The first one is approximately between the reversible potential and −100 mV *versus* RHE, and the second one is from −100 mV *versus* RHE up to the terminal point in the LSV. We took the first region as the most relevant because the eventual interference of gas-bubble is less pronounced. In the case of the other metals (practically all except Ru) after the onset potential, there was only one linear region. For metals whose onset potential is significantly more negative with respect to the reversible potential, the region of potential between the reversible potential and onset potential was usually disregarded. The reason for this was that extremely high values of the Tafel slope far exceed 120 mV/dec, indicating possible difficult intermediate adsorption, but most probably energetically demanding water reorientation/reconstruction, which definitely does not originate from HER. Tafel's approximation is generally used for out-of-equilibrium processes (minimum overpotential of $2.303RT/F \sim 60$ mV). If one analyzes the polarization curves of the four most active metals (Ir, Rh, Pt, and Pd), it can be observed that only the polarization curve on Ir reached a maximal targeted current density (25 mA cm^{-2}) at an overpotential smaller than $\sim$60 mV *versus* RHE. For all the other metals, the linear region of the Tafel plots is spreading toward larger overpotentials. Importantly, even in the case of Ir, the Tafel plot is linear despite the fact that the overpotential never reached $\sim$60 mV. This suggests that it is more realistic to use Tafel approximation than linear polarization for small overpotentials. Arrhenius plots originated from exchange current densities estimated at four different temperatures (20, 30, 40, and 50 °C) using previously explained Tafel's analysis. From the slope of the Arrhenius plots, activation energy was obtained, while the intercept was corresponding to the pre-exponential frequency factor. All Arrhenius plots (given now in Supporting Information) were linearly fitted with a correlation coefficient above 0.90, indicating strong correlation, except in the case of Cu and especially Ag, which are two points with the lowest confidence, because on these metals linear fit was not possible.

4.3. EIS Ohmic Drop Correction and Surface Roughness. Ohmic drop correction was conducted using electrolyte resistance extracted by EIS at open circuit conditions (OCP) and under-applied overpotential in the galvanostatic regime (current intensities of 0.01, 0.1, and 1 mA), because EIS based on potentiostatic polarization exhibited substantial noise. The employed alternate current (AC) perturbation was 10 mV using frequencies between 1 and 100 000 Hz. Supporting Information shows plots of the real component of impedance (Z') as a function of frequency, for four different conditions of galvanostatic polarization (0, 0.01, 0.1, and 1 mA) and four different temperatures (20, 30, 40, and 50 °C). It is interesting to observe that current density (at frequencies larger than 1000 Hz) had a minor influence on Ohmic resistance, despite the possible impact of gas bubbles. Our expectation was that with an increase of current, Ohmic resistance will also increase; however,

there was no significant trend in that case. At the same time, temperature change had a noticeable impact on Ohmic resistance. At 20 °C, Ohmic resistance was around 28 Ω; at 50 °C, it dropped to 20 Ω. This was very important to consider during Ohmic drop correction of LSV measurements. Double layer capacitance was not extracted due to the fact that without knowledge of the specific capacitance of every material (*i.e.,* usually done on single crystal materials that are not really relevant for polycrystalline materials with a substantial number of defects) usage of double layer capacitance for estimation of the active surface area is not appropriate. Second and most importantly, as discussed already in the text above, due to gas bubble blockage phenomena, the true challenge is the effective surface area. Briefly, considering roughness, flat polycrystalline electrodes were used, which were pretreated using the same procedure given above, so differences in roughness are expected to be minor. However, even if we could accurately determine the number of active sites for gas evolving electrodes, this is definitely not sufficient. What is relevant is the effective surface area that is somewhere between real area (defined by a total number of active sites) and geometric area. The effective surface area is the average fraction of the real surface area that is not covered by gas bubbles at a defined overpotential. We proposed in the past a methodology to estimate that quantity. However, the methodology conceals some weak points. To our knowledge, a reliable methodology for the determining effective surface area is yet to be developed; until then, every comparison or kinetic analysis of gas evolving electrodes done in the last 100 years is questionable. This is valid also for flat electrodes (not only for porous electrodes) because gas evolution depends on the hydrophilicity/hydrophobicity of a surface that can significantly vary on different metals, oxides, and so forth. Additionally, impedance data were collected using the Mott–Schottky operational mode where capacitance at 100 000 Hz is measured as a function of the applied potential to observe the difference in capacitance at conditions where no gas bubbles are generated and conditions of gas evolution (shown in Supporting Information). By observing this difference, one can get some insight into what fraction of the geometric area is blocked with gas bubbles. Noise was substantial in these experiments, so we report an example of it in Supporting Information. Noise was partially due the high frequency that was used to ensure negligible pseudo-capacitance and that we observed only double layer capacitance.

ASSOCIATED CONTENT

Supporting Information

The Supporting Information is available free of charge at https://pubs.acs.org/doi/10.1021/acscatal.2c02964.

LSV measurements, Arrhenius plots, selected impedance spectroscopy measurements and collection of kinetic parameters (PDF)

AUTHOR INFORMATION

Corresponding Author

Aleksandar R. Zeradjanin − *Max Planck Institute for Chemical Energy Conversion, 45470 Mülheim an der Ruhr, Germany;* orcid.org/0000-0002-0649-0544; Phone: +49-(0)208-306-3726; Email: aleksandar.zeradjanin@cec.mpg.de

Authors

Praveen Narangoda − *Max Planck Institute for Chemical Energy Conversion, 45470 Mülheim an der Ruhr, Germany*

Justus Masa − *Max Planck Institute for Chemical Energy Conversion, 45470 Mülheim an der Ruhr, Germany*

Robert Schlögl − *Max Planck Institute for Chemical Energy Conversion, 45470 Mülheim an der Ruhr, Germany; Fritz-Haber-Institut der Max-Planck Gesellschaft, 14195 Berlin, Germany*

Complete contact information is available at:
https://pubs.acs.org/10.1021/acscatal.2c02964

Author Contributions

The manuscript was written through the contributions of all authors. All authors have given approval for the final version of the manuscript.

Funding

Notes

The authors declare no competing financial interest.

REFERENCES

(1) Lewis, N. S.; Nocera, D. G. Powering the Planet: Chemical Challenges in Solar Energy Utilization. *Proc. Natl. Acad. Sci. U.S.A.* **2006**, *103*, 15729−15735.

(2) Katsounaros, I.; Cherevko, S.; Zeradjanin, A. R.; Mayrhofer, K. J. J. Oxygen Electrochemistry as a Cornerstone for Sustainable Energy Conversion. *Angew. Chem., Int. Ed.* **2014**, *53*, 102−121.

(3) Katsounaros, I.; Cherevko, S.; Zeradjanin, A. R.; Mayrhofer, K. J. J. Die Elektrochemie des Sauerstoffs als Meilenstein für eine nachhaltige Energieumwandlung. *Angew. Chem.* **2014**, *126*, 104−124.

(4) Zeradjanin, A. R.; Masa, J.; Spanos, I.; Schlögl, R. Activity and Stability of Oxides During Oxygen Evolution Reaction—From Mechanistic Controversies Toward Relevant Electrocatalytic Descriptors. *Front. Energy Res.* **2021**, *8*, 613092.

(5) Divanis, S.; Kutlusoy, T.; Ingmer Boye, I. M.; Man, I. C.; Rossmeisl, J. Oxygen Evolution Reaction: A Perspective on a Decade of Atomic Scale Simulations. *Chem. Sci.* **2020**, *11*, 2943−2950.

(6) Zeradjanin, A. R.; Polymeros, G.; Toparli, C.; Ledendecker, M.; Hodnik, N.; Erbe, A.; Rohwerder, M.; La Mantia, F. What Is the Trigger for the Hydrogen Evolution Reaction?—Towards Electrocatalysis beyond the Sabatier Principle. *Phys. Chem. Chem. Phys.* **2020**, *22*, 8768−8780.

(7) Ledezma-Yanez, I.; Wallace, W. D. Z.; Sebastián-Pascual, P.; Climent, V.; Feliu, J. M.; Koper, M. T. M. Interfacial Water Reorganization as a PH-Dependent Descriptor of the Hydrogen Evolution Rate on Platinum Electrodes. *Nat. Energy* **2017**, *2*, 17031.

(8) Zeradjanin, A. R.; Grote, J.-P.; Polymeros, G.; Mayrhofer, K. J. J. A Critical Review on Hydrogen Evolution Electrocatalysis: Re-Exploring the Volcano-Relationship. *Electroanalysis* **2016**, *28*, 2256−2269.

(9) Parsons, R. The Rate of Electrolytic Hydrogen Evolution and the Heat of Adsorption of Hydrogen. *Trans. Faraday Soc.* **1958**, *54*, 1053.

(10) Schilter, D. Electrocatalysis: Volcano Spews out Hot New Catalyst. *Nat. Rev. Chem.* **2018**, *2*, 0116.

(11) Koper, M. T. M. Analysis of Electrocatalytic Reaction Schemes: Distinction between Rate-Determining and Potential-Determining Steps. *J. Solid State Electrochem.* **2013**, *17*, 339−344.

(12) Koper, M. T. M. Thermodynamic Theory of Multi-Electron Transfer Reactions: Implications for Electrocatalysis. *J. Electroanal. Chem.* **2011**, *660*, 254−260.

(13) Koper, M. T. M. Activity Volcanoes for the Electrocatalysis of Homolytic and Heterolytic Hydrogen Evolution. *J. Solid State Electrochem.* **2016**, *20*, 895−899.

(14) Costentin, C.; Dridi, H.; Savéant, J.-M. Molecular Catalysis of H_2 Evolution: Diagnosing Heterolytic versus Homolytic Pathways. *J. Am. Chem. Soc.* **2014**, *136*, 13727−13734.

(15) Zagal, J. H.; Koper, M. T. M. Reactivity Descriptors for the Activity of Molecular MN4 Catalysts for the Oxygen Reduction Reaction. *Angew. Chem., Int. Ed.* **2016**, *55*, 14510−14521.

(16) Trasatti, S. Work Function, Electronegativity, and Electrochemical Behaviour of Metals. *J. Electroanal. Chem. Interfacial Electrochem.* **1972**, *39*, 163−184.

(17) Nørskov, J. K.; Bligaard, T.; Logadottir, A.; Kitchin, J. R.; Chen, J. G.; Pandelov, S.; Stimming, U. Trends in the Exchange Current for Hydrogen Evolution. *J. Electrochem. Soc.* **2005**, *152*, J23.

(18) Stamenkovic, V. R.; Fowler, B.; Mun, B. S.; Wang, G.; Ross, P. N.; Lucas, C. A.; Marković, N. M. Improved Oxygen Reduction Activity on Pt3Ni(111) via Increased Surface Site Availability. *Science* **2007**, *315*, 493−497.

(19) Quaino, P.; Juarez, F.; Santos, E.; Schmickler, W. Volcano Plots in Hydrogen Electrocatalysis—Uses and Abuses. *Beilstein J. Nanotechnol.* **2014**, *5*, 846−854.

(20) Exner, K. S. Hydrogen Electrocatalysis Revisited: Weak Bonding of Adsorbed Hydrogen as the Design Principle for Active Electrode Materials. *Curr. Opin. Electrochem.* **2021**, *26*, 100673.

(21) Exner, K. S. Paradigm Change in Hydrogen Electrocatalysis: The Volcano's Apex Is Located at Weak Bonding of the Reaction Intermediate. *Int. J. Hydrogen Energy* **2020**, *45*, 27221−27229.

(22) Exner, K. S. Does a Thermoneutral Electrocatalyst Correspond to the Apex of a Volcano Plot for a Simple Two-Electron Process? *Angew. Chem., Int. Ed.* **2020**, *59*, 10236−10240.

(23) Santos, E.; Quaino, P.; Schmickler, W. Theory of Electrocatalysis: Hydrogen Evolution and More. *Phys. Chem. Chem. Phys.* **2012**, *14*, 11224.

(24) Santos, E.; Pötting, K.; Schmickler, W. On the Catalysis of the Hydrogen Oxidation. *Faraday Discuss.* **2009**, *140*, 209−218.

(25) Exner, K. S. Why Approximating Electrocatalytic Activity by a Single Free-energy Change Is Insufficient. *Electrochim. Acta* **2021**, *375*, 137975.

(26) Zeradjanin, A. R. Frequent Pitfalls in the Characterization of Electrodes Designed for Electrochemical Energy Conversion and Storage. *ChemSusChem* **2018**, *11*, 1278−1284.

(27) Durst, J.; Siebel, A.; Simon, C.; Hasché, F.; Herranz, J.; Gasteiger, H. A. New Insights into the Electrochemical Hydrogen Oxidation and Evolution Reaction Mechanism. *Energy Environ. Sci.* **2014**, *7*, 2255−2260.

(28) Boodts, J. C. F.; Trasatti, S. Hydrogen Evolution on Iridium Oxide Cathodes. *J. Appl. Electrochem.* **1989**, *19*, 255−262.

(29) De Pauli, C. P.; Trasatti, S. Composite Materials for Electrocatalysis of O2 Evolution: IrO2+SnO2 in Acid Solution. *J. Electroanal. Chem.* **2002**, *538−539*, 145−151.

(30) Trueba, M.; Trasatti, S. P.; Trasatti, S. Electrocatalytic Activity for Hydrogen Evolution of Polypyrrole Films Modified with Noble Metal Particles. *Mater. Chem. Phys.* **2006**, *98*, 165−171.

(31) Narangoda, P.; Spanos, I.; Masa, J.; Schlögl, R.; Zeradjanin, A. R. Electrocatalysis Beyond 2020: How to Tune the Preexponential Frequency Factor. *ChemElectroChem* **2022**, *9*, No. e202101278.

(32) Omura, J.; Yano, H.; Watanabe, M.; Uchida, H. Electrochemical Quartz Crystal Microbalance Analysis of the Oxygen Reduction Reaction on Pt-Based Electrodes. Part 1: Effect of Adsorbed Anions on the Oxygen Reduction Activities of Pt in HF, HClO$_4$, and H$_2$SO$_4$ Solutions. *Langmuir* **2011**, *27*, 6464−6470.

(33) Chung, D. Y.; Lopes, P. P.; Farinazzo Bergamo Dias Martins, P.; He, H.; Kawaguchi, T.; Zapol, P.; You, H.; Tripkovic, D.; Strmcnik, D.; Zhu, Y.; Seifert, S.; Lee, S.; Stamenkovic, V. R.; Markovic, N. M. Dynamic Stability of Active Sites in Hydr(Oxy)Oxides for the Oxygen Evolution Reaction. *Nat. Energy* **2020**, *5*, 222−230.

(34) Spanos, I.; Masa, J.; Zeradjanin, A.; Schlögl, R. The Effect of Iron Impurities on Transition Metal Catalysts for the Oxygen Evolution Reaction in Alkaline Environment: Activity Mediators or Active Sites? *Catal. Lett.* **2021**, *151*, 1843−1856.

(35) Jerkiewicz, G.; Vatankhah, G.; Tanaka, S.; Lessard, J. Discovery of the Potential of Minimum Mass for Platinum Electrodes. *Langmuir* **2011**, *27*, 4220−4226.

(36) Strmcnik, D.; Uchimura, M.; Wang, C.; Subbaraman, R.; Danilovic, N.; van der Vliet, D.; Paulikas, A. P.; Stamenkovic, V. R.; Markovic, N. M. Improving the Hydrogen Oxidation Reaction Rate by Promotion of Hydroxyl Adsorption. *Nat. Chem.* **2013**, *5*, 300−306.

(37) Zeradjanin, A. R.; Ventosa, E.; Bondarenko, A. S.; Schuhmann, W. Evaluation of the Catalytic Performance of Gas-Evolving Electrodes Using Local Electrochemical Noise Measurements. *ChemSusChem* **2012**, *5*, 1905−1911.

(38) Zeradjanin, A. R.; Narangoda, P.; Spanos, I.; Masa, J.; Schlögl, R. How to Minimise Destabilising Effect of Gas Bubbles on Water Splitting Electrocatalysts? *Curr. Opin. Electrochem.* **2021**, *30*, 100797.

(39) Zeradjanin, A. R. Is a Major Breakthrough in the Oxygen Electrocatalysis Possible? *Curr. Opin. Electrochem.* **2018**, *9*, 214−223.

(40) Arikado, T.; Iwakura, C.; Tamura, H. Some Oxide Catalysts for the Anodic Evolution of Chlorine: Reaction Mechanism and Catalytic Activity. *Electrochim. Acta* **1978**, *23*, 9−15.

(41) Jakšić, M. M. Advances in Electrocatalysis for Hydrogen Evolution in the Light of the Brewer-Engel Valence-Bond Theory. *J. Mol. Catal.* **1986**, *38*, 161−202.

(42) Zeradjanin, A. R.; Narangoda, P.; Spanos, I.; Masa, J.; Schlögl, R. Expanding the Frontiers of Hydrogen Evolution Electrocatalysis—Searching for the Origins of Electrocatalytic Activity in the Anomalies of the Conventional Model. *Electrochim. Acta* **2021**, *388*, 138583.

(43) Gerischer, H. Mechanismus Der Elektrolytischen Wasserstoffabscheidung Und Adsorptionsenergie von Atomarem Wasserstoff. *Bull. Soc. Chim. Belg.* **2010**, *67*, 506−527.

(44) He, Z.; Chen, Y.; Santos, E.; Schmickler, W. The Pre-exponential Factor in Electrochemistry. *Angew. Chem., Int. Ed.* **2018**, *57*, 7948−7956.

(45) Teschner, D.; Novell-Leruth, G.; Farra, R.; Knop-Gericke, A.; Schlögl, R.; Szentmiklósi, L.; Hevia, M. G.; Soerijanto, H.; Schomäcker, R.; Pérez-Ramírez, J.; López, N. In Situ Surface Coverage Analysis of RuO2-Catalysed HCl Oxidation Reveals the Entropic Origin of Compensation in Heterogeneous Catalysis. *Nat. Chem.* **2012**, *4*, 739−745.

(46) Marković, N. M.; Grgur, B. N.; Ross, P. N. Temperature-Dependent Hydrogen Electrochemistry on Platinum Low-Index Single-Crystal Surfaces in Acid Solutions. *J. Phys. Chem. B* **1997**, *101*, 5405−5413.

(47) He, Z.-D.; Wei, J.; Chen, Y.-X.; Santos, E.; Schmickler, W. Hydrogen Evolution at Pt(111)—Activation Energy, Frequency Factor and Hydrogen Repulsion. *Electrochim. Acta* **2017**, *255*, 391−395.

(48) Zeradjanin, A. R.; Vimalanandan, A.; Polymeros, G.; Topalov, A. A.; Mayrhofer, K. J. J.; Rohwerder, M. Balanced Work Function as a Driver for Facile Hydrogen Evolution Reaction—Comprehension and Experimental Assessment of Interfacial Catalytic Descriptor. *Phys. Chem. Chem. Phys.* **2017**, *19*, 17019−17027.